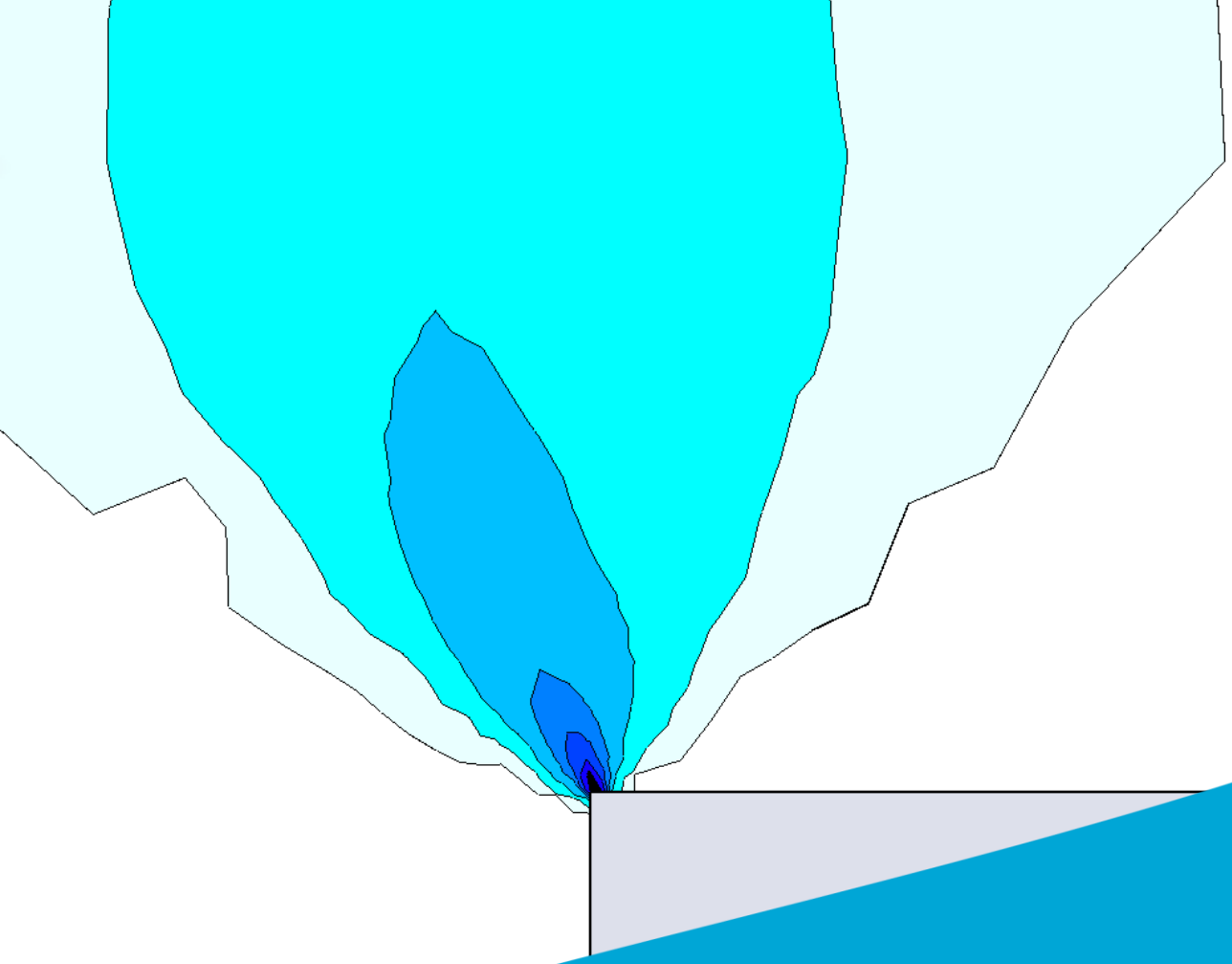

Stress Concentrations

Impact Analysis on the Linear Elastic and Plastic Strain Relation When Adding Reinforcement to an Opening in a Steel Beam

Author: David de Deugd
Date: 19th of June 2026

TU Delft

Stress Concentrations

Impact Analysis on the Linear Elastic and Plastic Strain Relation When Adding Reinforcement to an Opening in a Steel Beam

By

David de Deugd
5805805

In partial fulfilment of the requirements for the degree of:

Bachelor of Science
in Civil Engineering

at the Delft University of Technology,

Thesis committee:

Dr. ir. P.C.J. Hoogenboom	TU Delft, supervisor 1
Dr. F. Kavoura	TU Delft, supervisor 2

TU Delft

Preface

This thesis report is part of my bachelor's final project through which I will complete the bachelor program Civil Engineering at Delft University of Technology. This report looks at the impact of adding reinforcement to a steel beam with an opening in its web. Throughout this final project I familiarized myself with SCIA Engineer and how to perform plastic analysis using this program. As much as attempting to learn how to do so felt frustrating at times, I did ultimately enjoy the process and gained a greater appreciation for the capabilities of structural modelling software. I hope this report provides a clear manual or potential methodology for other engineers who are interested in doing a similar analysis.

A lot of thanks goes out to my supervisors Pierre Hoogenboom and Florentia Kavoura for guiding me through this final project.

Summary

When introducing an opening to the web of a beam, stresses will concentrate around the opening. Depending on the shape of the hole these stress concentrations can be described differently. For rectangular openings this stress concentration can reach very large values and even become singular due to the sudden geometry change at the corner. Common practice is to reinforce such an opening by welding a metal plate along the top- and bottom side of the opening.
This report aims to understand the impact of adding such reinforcement on the yield area around the opening when the steel fails for two steel types (S235JR & S355JR) and three increasingly more refined mesh configurations. This analysis will be done in SCIA Engineer using a 2D Finite Element Analysis.

To define the scope of this research, the following the research question has been defined:

- "*What is the impact of applying reinforcement to a rectangular opening in a steel beam on the yield area and plastic strain at failure?"*

This research question will be supported by the following sub questions:

- "*How large can the yield area and unity check value be before failure happens for both models and each mesh configuration?"*
- *"What is the difference in yield area between models for each mesh configuration?"*
- *"What is the difference in plastic behaviour between models for each mesh configuration?"*
- *"What mesh size provides sufficiently accurate linear elastic calculation results such that failure can be determined without a nonlinear calculation?"*

This analysis was performed by creating two models. The first model being a simple model with no reinforcement and the second model having reinforcement added to it. These models are created by using 2D plate- and wall elements to recreate a beam, after which a rectangular opening was created in the middle point of the web. The beam is supported by 4 hinges, of which 3 allow for longitudinal displacement. Finally, a trapezium load was applied along the topside of the beam such that the greatest stress is applied to a corner of the opening.
When applying a load such that the plastic strain would become critical, both models using S235JR steel would yield across the entire cross section creating a plastic hinge. The models using S355JR did not yield across the entire cross section, instead a local yield area was identified around the critical corner of the opening. Comparing the yield area and plastic behaviour of the models showed that the yield area decreased by 80%, becoming much more concentrated. The plastic strain only became critical in the most refined mesh configuration of each model. Between the two models, the plastic strain reached a greater value in a larger area before failing, i.e. the plastic strain was spread out more across the plastic zone when failing.
These findings imply that applying such reinforcement allows a beam to have a greater span and opening size compared to an unreinforced model without getting a plastic hinge. Additionally, the reinforced model showed greater stresses in areas other than the critical corner before failing. Extrapolating this result would suggest that the opening would no longer be critical upon adding sufficiently large reinforcement. Finally, the difference in results for the yield area between the least refined mesh configuration and the two more refined mesh configurations was very significant. The discrepancy between the other two mesh configurations was much smaller. From this it can be concluded that the medium mesh refinement is sufficiently accurate to determine whether or not the steel will fail. Do note however, that for solid conclusions on the actual size of the yield area in relation to whether or not the steel fails, more research is needed.

Contents

Preface i

Summary ii

1 Introduction 1
- 1.1 Problem Analysis 1
- 1.2 Approach 1

2 Literature 2
- 2.1 Linear Elastic Calculations 2
  - 2.1.1 Assumptions 2
  - 2.1.2 Stress Concentration Factors 2
- 2.2 Finite Element Method 3
  - 2.2.1 Definitions 3
  - 2.2.2 Finite Element Analysis 3
  - 2.2.3 Singularity 4
- 2.3 Plastic Calculations 4
  - 2.3.1 Von Mises Yield Criterion 4
  - 2.3.2 Associated Flow Rule 4
  - 2.3.3 Coupled Elasto-Plasticity and Constitutive Equations 4
  - 2.3.4 Material Failure 5

3 Approach 6
- 3.1 Plastic Analysis in SCIA Engineer 6
  - 3.1.1 Plastic Analysis Prerequisites 6
  - 3.1.2 Modelling the Beam 7
  - 3.1.3 Mesh Refinement 7
  - 3.1.4 Nonlinear Calculations 7
- 3.2 Models 8
  - 3.2.1 Model 1: Simple Model 9
  - 3.2.2 Model 2: Simple Model with Reinforcement 9

4 Results 10
- 4.1 Results Interpretation 10
- 4.2 Model Results 11

5 Discussion 16
- 5.1 Model and Methodology 16
- 5.2 Future Works 16

6 Conclusion 17

7 References 19

Appendix A: Steel Properties 21

Appendix B: Mesh Grids 22

Appendix C: Yield Area & Plastic Strain of the Entire Beam 23

Appendix D: Yield Area Division & Results 25

1 Introduction

1.1 Problem Analysis

In construction, it is commonplace for utility-related items, such as cables or tubes, to pass through a steel beam to reduce story height. Creating an opening in a steel beam necessitates careful consideration of the beam's structural integrity. The removal of material increases the risk of geometric instabilities as well as stress concentrations around the opening. A common solution is to stiffen the opening by welding a metal reinforcement plate around the opening, along the top and bottom side for example.

This thesis aims to analyse the impact of adding such reinforcement on the yield area around the opening, as well as the associated plastic strain behaviour at failure. The impact will be analysed by comparing a linear elastic analysis and a nonlinear plastic analysis using SCIA Engineer to allow for easy replication.

The main research question posed in this thesis is:

- "*What is the impact of applying reinforcement to a rectangular opening in a steel beam on the yield area and plastic behaviour at failure?"*

Supporting this research question are the following sub questions:

- "*How large can the yield area and unity check value be before failure happens for both models and each mesh configuration?"*
- *"What is the difference in yield area at failure between models for each mesh configuration?"*
- *"What is the difference in plastic behaviour between models for each mesh configuration?"*
- *"What mesh size provides sufficiently accurate linear elastic calculation results such that failure can be determined without a nonlinear calculation?"*

1.2 Approach

This report will first provide some background information via a literature study in chapter 2, examining stress concentration factors, the Finite Element Method and plastic behaviour of steel. Chapter 3 will provide a brief explanation on how to perform plastic analysis using SCIA Engineer. Following this will be an explanation on the models used in this thesis as well as what calculation protocols were used. Chapter 4 will display the results found using the aforementioned models after which a discussion and conclusion will be presented in chapter 5 and 6 respectively.

2 Literature

This chapter explores how an opening in a steel plate affects stress behaviour, how the Finite Element Method can be applied to steel plates and how the plastic behaviour of steel plates can be described.

2.1 Linear Elastic Calculations

2.1.1 Assumptions

A linear elastic state assumes small deformations, a linear relation between the applied load and resulting strain and a fully elastic response when the applied load is removed. These assumptions are valid as long as the applied loads do not cause yielding stresses across large structural elements. If the resulting stresses surpass the yield stress, the associated strain no longer behaves linearly, which invalidates the linear elastic assumption.

2.1.2 Stress Concentration Factors

When observing stresses around a hole subject to loading, a significant increase in stress near the edges of the hole can be observed. This increased stress state around the edges is a stress concentration and can be described by a stress concentration factor K_t, which relates the local peak stress to the nominal stress of the material. These stress concentrations occur due to a sudden change in geometry causing stress lines to converge as shown in Figure 1 (Crawford, 1998). This increase in stress diminishes significantly as the distance from the edge of the hole increases and becomes negligible when this distance is equal to or greater than twice the diameter of the hole as shown in Figure 2 (Vellaichamy, Vignesh, Indhumathi, & Senthilkumar, 2020).

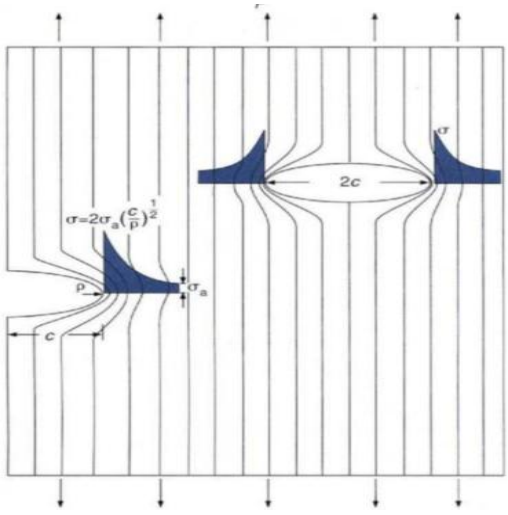

Figure 1: Stress concentration around surface (left) and internal (right) cracks (Ohring, 1995)

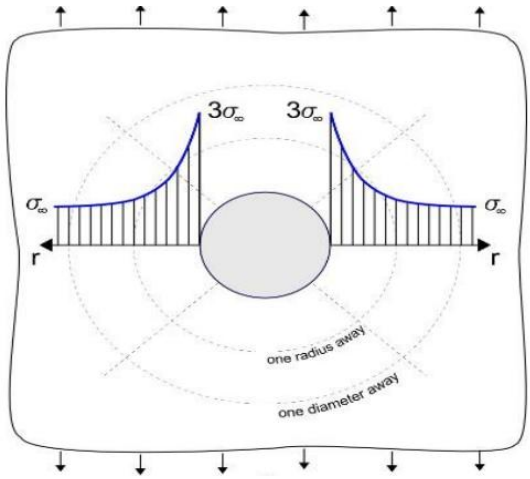

Figure 2: Stress concentration around a hole (Vellaichamy, Vignesh, Indhumathi, & Senthilkumar, 2020)

A common equation for K_t in the case of an internal hole is defined as:

$$K_t = 1 + 2\sqrt{a/r} \tag{2.1}$$

Where *a* is half the length of the hole and r is the radius of the curve. When the hole is a perfect circle such that *a* equals *r*, the value for K_t becomes 3, which results in a peak stress of 3 times the nominal stress as shown in Figure 2.

This however only holds true for this specific scenario. In general the value of K_t is a function of multiple variables: the geometry of the hole (the shape, size and orientation of the hole with respect to loading plane (Figure 3)), the type of loading (axial, bending, torsion) and the sharpness of the angles of the hole (Figure 4). In Figure 4, the value for K_t (SCF in the graph) is expressed as a polynomial function of the ratio between the side length of the opening and the radius of the curved corners. From this graph one can derive that as this ratio increases, i.e. the radius of the corner decreases, the value for K_t increases as well.

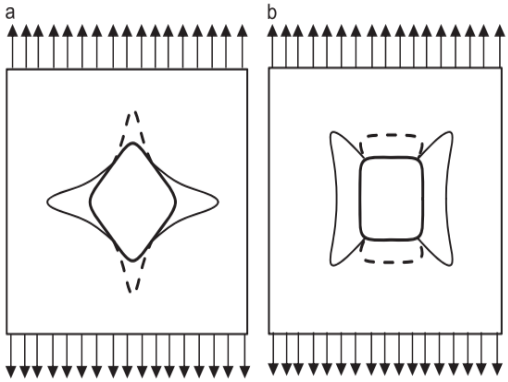

Figure 3: Stress distribution around square hole in rotation angle of: (a) zero (b):45° (Jafari & Ardalani, 2016)

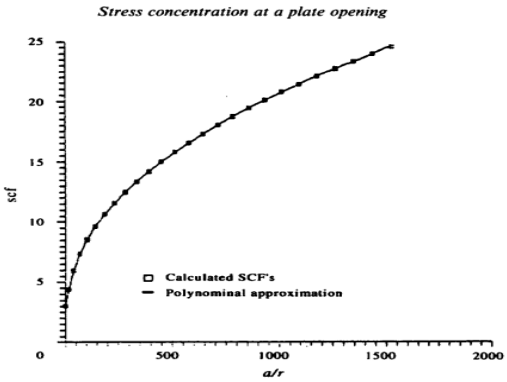

Figure 4: Corner SCF as a function of the relative corner radius of curvature (Motok, 1997)

2.2 Finite Element Method

2.2.1 Definitions

The Finite Element Method (FEM) is a numerical method, a mathematical process during which the solution to a problem is approximated rather than being solved analytically by means of finite computational processes. Such a method is used when the exact solution either is impossible or prohibitively difficult to find (Vuik, Vermolen, van Gijzen, & Vuik, 2023). In the case of structural mechanics, the FEM is used to solve a set of equilibrium equations by approximating continuous field variables at nodes. These field variables are nodal displacements and loads/stresses.

These nodes are discrete points in the domain (e.g. a beam). The lines connecting these nodes are called elements. In 2D these elements take simple shapes (e.g. triangles or quadrilaterals) and solids in 3D. The nodes and elements together form a mesh as shown in Figure 5. (Chen, 2020).

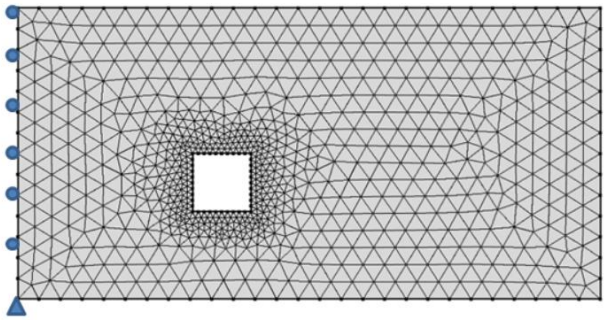

Figure 5: Mesh Grid (Sönnerlind, 2015)

2.2.2 Finite Element Analysis

Using the Finite Element Method to analyse a system is called a Finite Element Analysis (FEA). The first step in performing such an analysis is to construct a mesh. As mentioned, the actual mesh generation is performed by the program that is used, however, this does require a certain element shape and size. To verify whether or not the resulting mesh is sufficiently refined, an iterative process can be used: by repeating the calculation using half the element size one can conclude a mesh is valid when no significant change in results can be observed between operations (Hoogenboom, Notes on Shell Structures, 2024). Using a more refined mesh will yield more “accurate” results. This however is not the case for the entire domain. At certain nodes the calculated stresses (and consequently strains) can become singular.

2.2.3 Singularity

In mathematics, “a singularity is a point at which an equation, surface, etc., blows up or becomes degenerate” (Trott, 2026). In the context of structural engineering a singularity is a point of the mesh where the local stresses are unbounded and can theoretically become infinite as the mesh becomes more refined (Sönnerlind, 2015). This singularity is merely a numerical result of assuming a linear elastic state material. In reality, the material will yield in this point and redistribute the stresses it is subjugated to (Crawford, 1998). Such singularities can occur due to the application of a point load, re-entrant corners, point supports and where line supports stops (Hoogenboom, Notes on Shell Structures, 2024). A quick way to verify this is to look at equation (2.1), when the radius nears zero, the value for K_t approaches infinity and therefore becomes singular resulting in an increasingly larger stress in the node.

There are multiple ways to avoid unrealistic stresses in a corner. One of such methods is to assume that the corner is not perfectly sharp but instead has a finite radius. Locally this will limit the calculated stresses. However, this approach will still not yield accurate results in a linear elastic model as the calculated stresses will far exceed yielding limits (Hoogenboom, Piekspanningen in eindige-elementenberekeningen, 2007). Hence when analysing a physical domain such as a beam with an opening it is up to the engineer to validate results such that occurring singularities are properly accounted for.

2.3 Plastic Calculations

When a linear elastic calculation yields stresses significantly larger than the yield stress of the material the results do not reflect reality, instead the material will yield locally. This is when plastic calculations are required to determine deformations in the material.

2.3.1 Von Mises Yield Criterion

According to the Von Mises Yield Criterion, a material will start to yield once the Von Mises stress reaches the yield stress. This Von Mises stress can be computed according to:

$$\sigma_E = \sqrt{\frac{1}{2}[(\sigma_{11} - \sigma_{22})^2 + (\sigma_{22} - \sigma_{33})^2 + (\sigma_{33} - \sigma_{11})^2 + 6 \times (\sigma_{12}^2 + \sigma_{23}^2 + \sigma_{31}^2)]} \tag{2.2}$$

Once this threshold is reached, steel will start to behave nonlinearly and undergo plastic deformation.

2.3.2 Associated Flow Rule

According to the associated flow rule, the plastic strain increments occur in a direction normal to the yield surface. This implies that the shape of the yield surface is not affected by plastic deformation (Yoshida, 2017). This rule does not always hold true, as is the case for rocks and soil, for metals however it has been empirically verified through many experiments that this rule does apply (Kelly, 2010). This rule can therefore be applied to the study of ductile materials while yielding.

2.3.3 Coupled Elasto-Plasticity and Constitutive Equations

According to Lemaitre 1985a, when properly addressing the impact of plastic deformations, a coupling between the constitutive equations of stress and damage is to be assumed. Ductile damage can be described as the development of micro-cracks and micro-cavities creating surfaces of separation causing reduced rigidity of the material. Thus, from a physical standpoint it makes sense to assume that as damage increases the elasticity modulus and any plastic strain-hardening decreases. This also highlights the importance of using couple constitutive equations. If a material is close the failure, calculations using an uncoupled system would yield large errors.

Lemaitre also defines a scalar *D,* which describes the area of a material that resists the imposed stress. For such a scalar to exist, it is assumed that the damage is isotropic, i.e. the reduction of stiffness is uniform in all directions. Doing so allows the following relation:

$$\delta S_{resist} = \delta S(1 - D) \qquad (2.3)$$
$$0 \leq D \leq 1$$

Where δS is the area of a finite volume element.

The local stress and strain are directly related to this new effective area and can be described as such:

$$\tilde{\sigma} = \frac{\sigma}{1 - D} \qquad (2.4)$$

$$\varepsilon_e = \frac{\tilde{\sigma}}{E} = \frac{\sigma}{(1 - D)E} \qquad (2.5)$$

Where E is the Young's Modulus of the material and ε_e the elastic strain.

The new local stress derived in (2.4) allows the plastic strain ε_p to be described as:

$$\varepsilon_p = \left(\frac{\tilde{\sigma}}{K}\right)^M \qquad (2.6)$$

Where K and M are material coefficients.

When the material sustains damage such that D reaches a critical value, D_c, where the volume element fails.

2.3.4 Material Failure

As described, plastic deformation causes damage and therefore influences the scalar *D*. This results in an iterative process where the increase in plastic strain increases the value of *D* resulting in further plastic strain. This process continues until the material fails. How this process exactly unfolds depends on the (assumed) state of the material, e.g. a perfectly plastic state will see no variation in nominal stress throughout this process.

In structural engineering it is preferred to prevent any macro-cracks from happening in metals. According to Lemaitre 1985b, the critical value of *D*, D_c, where the material will start to show macro-cracks, is defined as:

$$D_c = \frac{K^2}{2ES_0}(\varepsilon_R - \varepsilon_D) \qquad (2.7)$$

Where ε_D and ε_R are the strain at the damage threshold and failure respectively and S_0 a factor dependent on the material and temperature.

The strain at which various steels fail on large scale is shown in the stress-strain curve in Figure 6. This figure shows the stress-strain curve in a tensile stress test which will be used to determine when the material will yield and fracture. Note that what would be considered the failure strain might not be the critical strain due to the softening of the material right before fracture. Assuming continued load, the steel will inevitably break once this softening starts to occur.

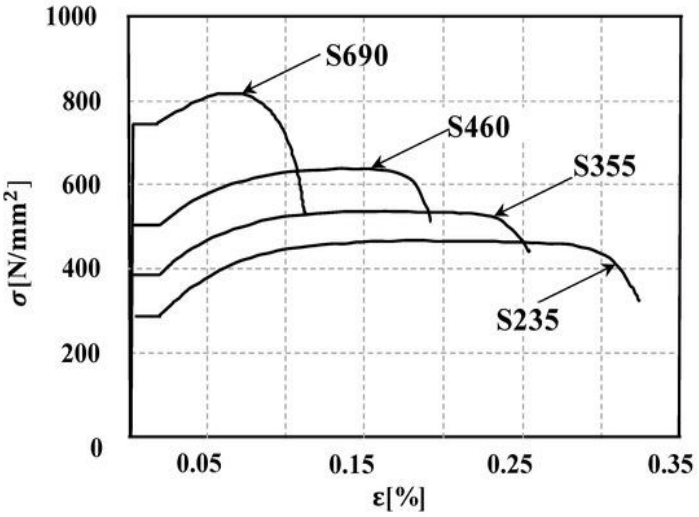

Figure 6: Stress-Strain Curve for various Steels (Li, Lee, & Cai, 2023)

3 Approach

This chapter explains the prerequisites to performing plastic analysis using SCIA Engineer after which the different models will be addressed.

3.1 Plastic Analysis in SCIA Engineer

3.1.1 Plastic Analysis Prerequisites

Performing plastic analysis on a metal plate using SCIA Engineer (SCIA) requires the following functionalities to be selected: '**Nonlinearity**' and '**General Plasticity**' as shown in Figure 7.

Additionally, the material behaviour of the steel must be set to '**Isotropic Elastic-Plastic, Von Mises**'. Depending on the accuracy of the model strain hardening can be selected. Both shown in Figure 9. To ensure that the coordinates of the finite element nodes are displayed sufficiently accurate changing the amount of displayed decimals from 3 to 5 can be crucial. This can be done in '**Unit Set**' property page, under '**Unit Dialog**', '**Geometry**' go to '**Length**'. The final result is shown in Figure 8.

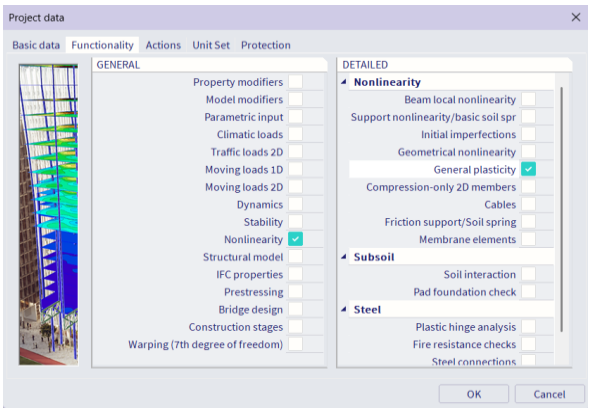

Figure 7: Functionality Selection

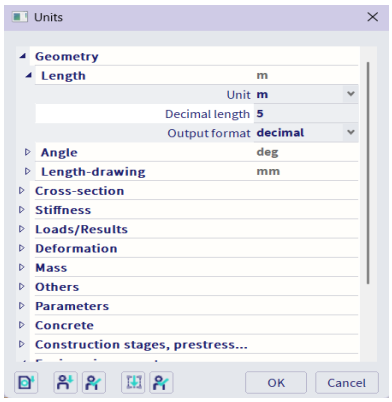

Figure 8: Decimal Length

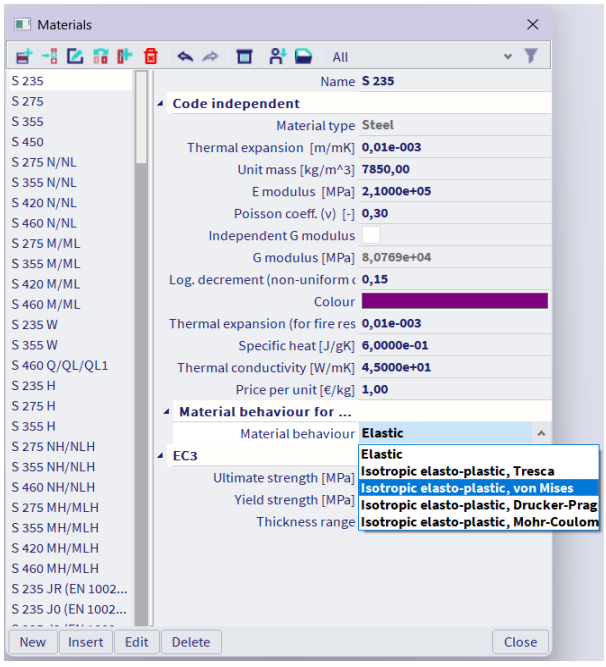

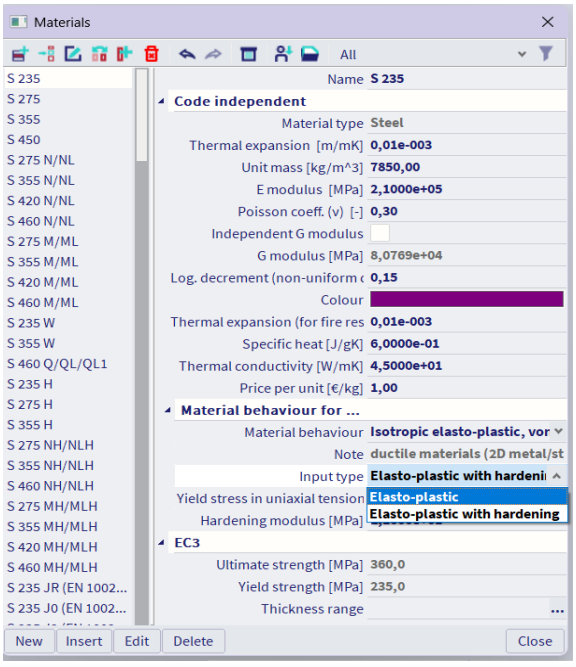

Figure 9: Selecting Material Properties

3.1.2 Modelling the Beam

Plastic analysis in SCIA requires 2D structural elements. Therefore the beam will be modelled using 2D plates and walls for the web and flanges. Note that the flanges should be modelled as two thin plates each of which are connected to the web as shown in Figure 10 such that SCIA automatically recognises that these elements are connected. The opening will be created using the option '**Opening on 2D**'.

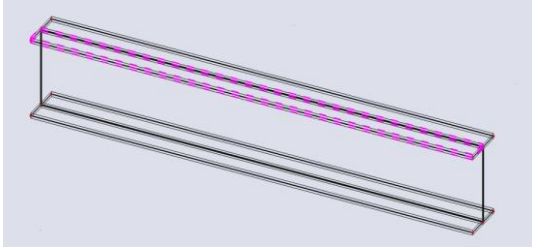

Figure 10: Flange & Web Connection

Hinged supports are added to each of the four corners of the web. One of the bottom supports must not allow any translation in x-, y- and z-directions. The other 3 supports must allow translation in the longitudinal direction of the beam. See Figure 11.

Finally a '**Line Load on 2D Edge**' is added along the centre of the web and combined with the self-weight load using nonlinear combinations.

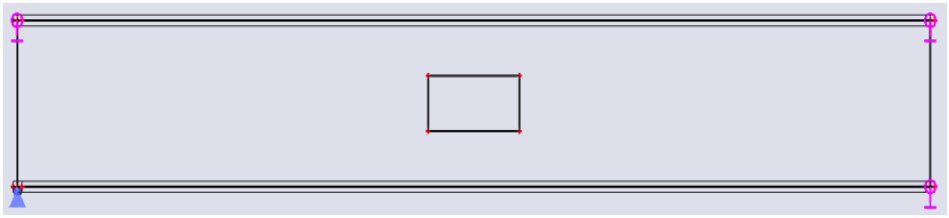

Figure 11: Beam Supports



3.1.3 Mesh Refinement

In SCIA there are two ways to refine the mesh. One is to adjust the average element size when calculating. The other method is to use mesh refinement options such as '**Edge Mesh Refinement**' and '**Node Mesh Refinement**'. To properly analyse plastic deformation, a sufficiently refined mesh around the corner nodes and edges of the opening is crucial.

3.1.4 Nonlinear Calculations

SCIA can perform nonlinear calculations using multiple iterative methods: 'Newton-Raphson', 'Modified Newton-Raphson', 'Picard' and Picard and Newton-Raphson'. For high accuracy the Newton-Raphson method can be applied. If the results from this method do not converge, Picard can be used to find results (SCIA Engineer, n.d.-a). The Newton-Raphson Method calculates the effects of the applied load(s) using increments, with each increment an amount of iterations is used to achieve converging results. To increase the accuracy of this method the number of increments and the number of iterations can be increased (SCIA Engineer, n.d.-b).

This report only considers small deformations under the assumption that the plastic strain in the corners of the opening will be the governing failure mechanism. Situations where this is not the case, e.g. instabilities due to geometrical nonlinearity (2nd order effect), are neglected.

3.2 Models

The model will have the dimensions as shown in Table 1. These dimensions are chosen to emulate an actual common beam in terms of height, thickness and width.

h	500 [mm]
b	200 [mm]
t_{flange}	16 [mm]
t_{web}	10,2 [mm]
L	5 [m]
$h_{opening}$	200 [mm]
$b_{opening}$	400 [mm]

Table 1:Beam and Opening Dimensions

Each model will be analysed using both S235JR and S355JR steel to better understand the impact of yield strength and ductility. The exact properties as denoted in SCIA are shown in appendix A. All models will be subjected to a trapezium load spanned across half the beam with its peak value being in the centre of the beam as shown in Figure 13. Reason for applying a trapezium load is to minimise the stress on the beam while still achieving failure in the corners of the opening.

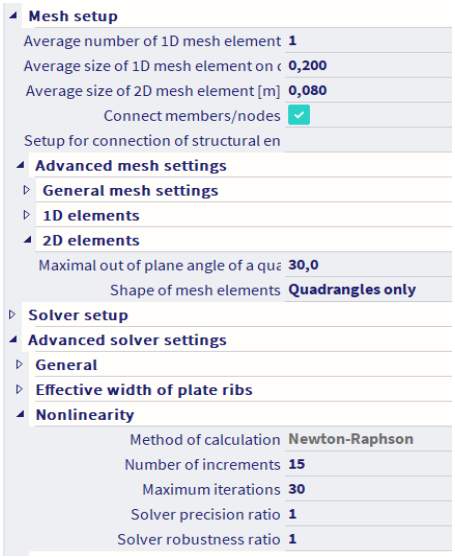

Figure 12: Mesh Setup and Advanced Solver Settings

Finally the impact of mesh refinement on the yield surface and plastic deformation for each model will be calculated with an increasingly more refined mesh. As this report primarily concerns itself with the accuracy around the opening and to limit the calculation efforts, the average mesh element size will be roughly 8 times the thickness of the web, i.e. 0,08 m. The used FE analysis mesh setup and solver settings are shown in Figure 12. Additionally the node and edge refinements will be increased twice per model to analyse the impact of mesh refinement on the relation between the yield surface and plastic deformation. The initial mesh will have an estimated mesh size approximately equal to the web thickness (10,2 mm). Note that the mesh will not be refined near the supports as it is assumed that this is not critical. The mesh refinements as noted in Table 2 will be applied in each of the models. For the final mesh refinement the element size near the corners will roughly be equal to the fillet radius resulting from a laser cut made in the metal. This fillet radius will have a minimum size equal to the kerf width (the width of the cut made in the material) of the used laser. This kerf width ranges from 0,1 to 0,3 mm (Lee, 2023). Using a more refined model would no longer yield realistic results. The final mesh configurations will be shown in Appendix B.

Refinement #	*Node Radius [m]*	*Node Ratio*	*Edge Size [m]*
1	0,05	0,1	0,05
2	0,05	0,05	0,02
3	0,05	0,005	0,002

Table 2: Mesh Refinements

3.2.1 Model 1: Simple Model

The first model will be a simple model with no reinforcement as shown in Figure 13. The mesh refinements are applied as is shown in Figure 14, the resulting mesh around the corner nodes is shown in Figure 15. Note that from top to bottom the mesh becomes more refined. The edge refinement on the third beam is applied the exact same way as is the other two beams, but due to the size it is hardly visible. The applied trapezium loads have maximum values of 372 and 446 kN/m for S235JR and S 355JR respectively.

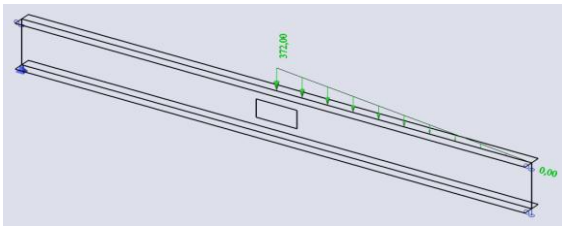

Figure 13: Model 1

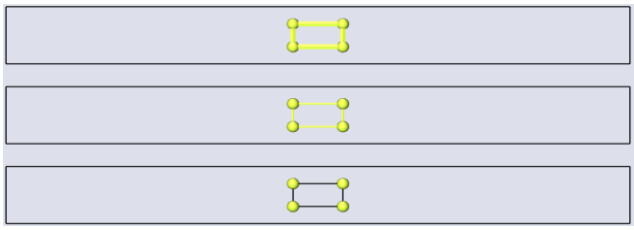

Figure 14: Model 1, Mesh Refinements

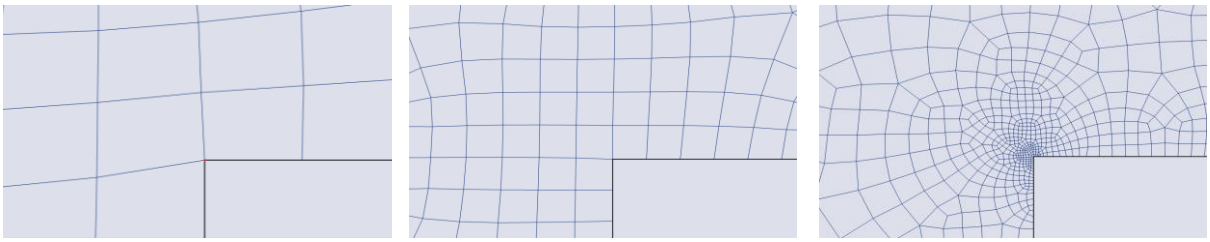

Figure 15: Model 1, Mesh Configuration at Corner Node for each Refinement Level

3.2.2 Model 2: Simple Model with Reinforcement

For the second model two small metal plates will be added to the top and bottom edge of the opening. The reinforcement plates on both sides have a thickness equal to one time the web's thickness, i.e. 10,2 mm. These plates have a height equal to 25 mm and protrude 100 mm beyond the edge of the opening. These additional plates will be modelled using the '**Subregion on 2D**' option. In reality these plates would be welded on, however in this case the reinforced areas will not be critical and will therefore not be modelled realistically. The model is shown in Figure 16. Due to the applied reinforcement the beam could start to fail near different corners of the reinforcement, therefore the mesh will be refined in each of the corners as shown in Figure 17. The applied trapezium loads have maximum values of 415 and 500 kN/m for S235JR and S355JR respectively.

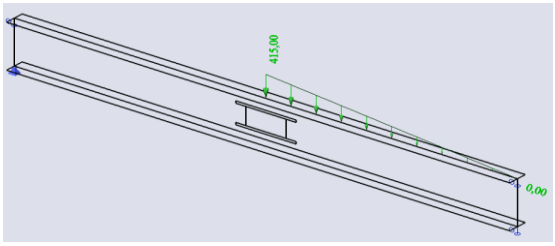

Figure 16: Model 2

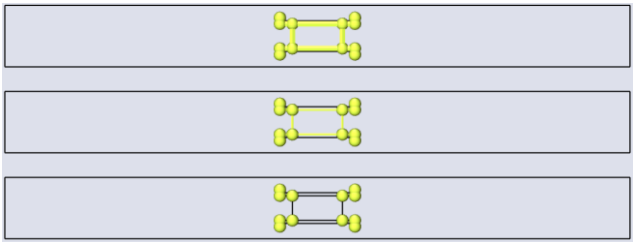

Figure 17: Model 2, Mesh Refinements

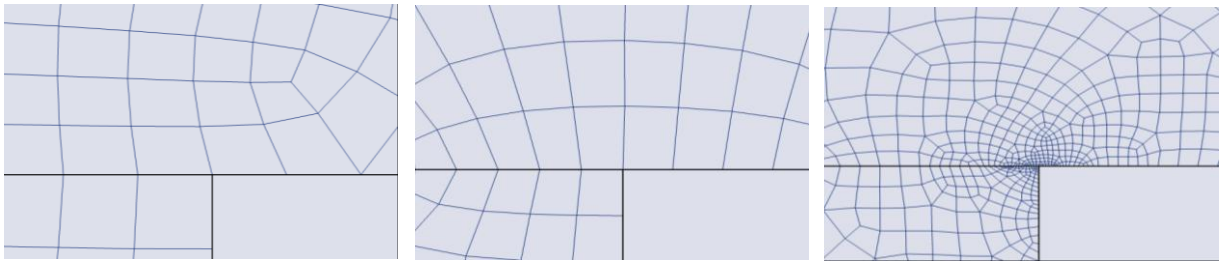

Figure 18: Model 2, Mesh Configuration at Corner Node for each Refinement Level

4 Results

This chapter presents the collected results from the linear elastic and nonlinear plastic analyses.

4.1 Results Interpretation

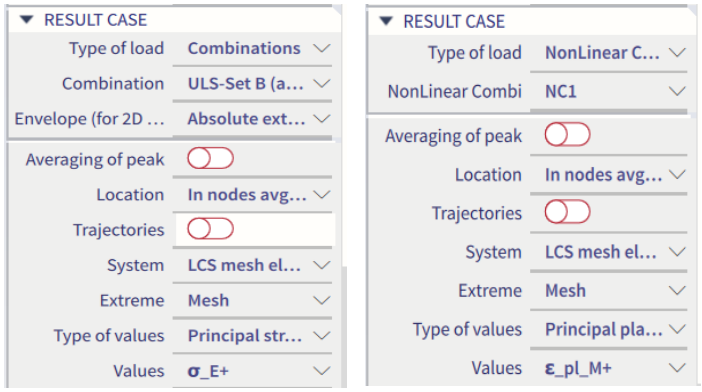

Figure 19: Result Cases for Stress (Left) and Plastic Strain (Right)

For each model, the equivalent stress distribution σ_E and plastic strain $\varepsilon_{pl,M}$ of the entire beam for both steel grades are shown in Appendix B. The result cases shown in Figure 19 are used to display the results. On the left the linear elastic calculation is displayed using the '**In Nodes Avg on Macro**', this provides the smoothest gradient along each element. On the right the nonlinear plastic calculation is shown using the same results location. The reason for only showing the equivalent plastic strain is that the elastic strain of metal can be considered sufficiently small relative to the plastic strain as can be seen in Figure 6. From the same figure it can be observed that the steel will fail (i.e. start to soften and fail) at roughly 30% and 23% strain for S235JR and S355JR respectively. Therefore the critical strain in the results will be as such.

For each model, the area in which the stress exceeds the yield stress will be calculated. SCIA 26.0 appears unable to export the geometry data of the finite elements in a way to get a numeric surface area of the yielding area. Instead a graphical approach will be used to estimate this area. By changing the view settings for all entities it is possible to see the node labels (Figure 20). When using the '**In Nodes Avg**' result case option, changing the extreme to '**Mesh**' and opening the results table, each node will be listed with its label, geometric properties and calculated values (Figure 21). By exporting this table to Excel and using the surface area equation as shown in 4.1 it is possible to manually find the surface area of any specific element. Unfortunately it is not possible to find connectivity between these nodes to automate this process across the entire yielding surface.

$$A = \frac{1}{2}\left|(x_1y_2 + x_2y_3 + x_3y_4 + x_4y_1) - (x_2y_1 + x_3y_2 + x_4y_3 + x_1y_4)\right| \tag{4.1}$$

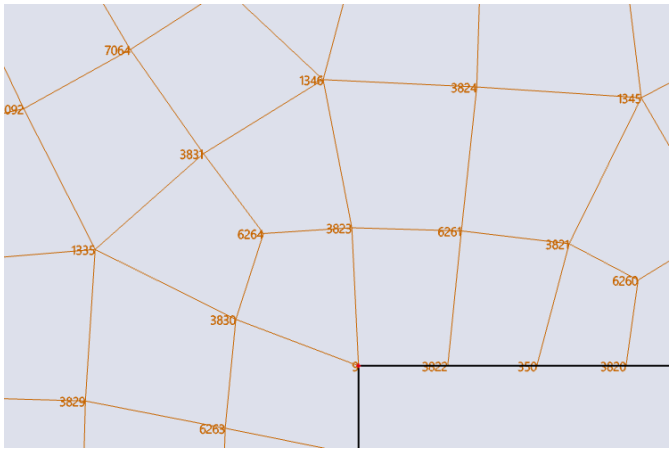

Figure 20: Node Labels

RESULTS TABLE

	Mesh	x [m]	y [m]	z [m]	σE+ [MPa]
		[5;5;4]		[-3,5;-3,68]	>355
1	Node: 9	5,20000	0,00000	-3,65000	3716,9
2	Node: 9	5,20000	0,00000	-3,65000	5017,9
3	Node: 330	5,26800	0,00000	-3,65000	359,9
4	Node: 331	5,26400	0,00000	-3,65000	369,9
5	Node: 332	5,26000	0,00000	-3,65000	380,1
6	Node: 333	5,25600	0,00000	-3,65000	391,2
7	Node: 334	5,25200	0,00000	-3,65000	402,0
8	Node: 335	5,24800	0,00000	-3,65000	413,7
9	Node: 336	5,24400	0,00000	-3,65000	426,8
10	Node: 337	5,24000	0,00000	-3,65000	440,9
11	Node: 338	5,23600	0,00000	-3,65000	457,1
12	Node: 339	5,23200	0,00000	-3,65000	474,3
13	Node: 340	5,22800	0,00000	-3,65000	366,2
14	Node: 340	5,22800	0,00000	-3,65000	494,4
15	Node: 341	5,22400	0,00000	-3,65000	384,5
16	Node: 341	5,22400	0,00000	-3,65000	519,1
17	Node: 342	5,22000	0,00000	-3,65000	407,5

Figure 21: In Nodes Avg Results Table

The graphical method used to determine the yielding area is to use the '**In Centres**' results case option and divide the yielding area into areas with a different average element size. Exporting the node data shown in Figure 21 to Excel, the average surface area of each element size type can be calculated. Then, by counting the amount of elements per element type, the total area of the yielding surface can be estimated.

4.2 Model Results

In the figures below the area in which the equivalent stress surpasses the yield stress (marked in red) of the material and plastic strain are displayed for both models with S235JR and S355JR steel. The area in which the material reaches critical plastic strain is coloured black, areas where no plastic strain occurs at all is shown in white. Figure 22 and Figure 23 show the equivalent stress around the opening for both models. In Figure 24, Figure 25, Figure 26 and Figure 27 The equivalent stress area and plastic strain are shown for the area where the steel will fail first. The yielding area is zoomed out compared to the equivalent plastic strain to capture the entire yielding area while also capturing the detail of the plastic strain.

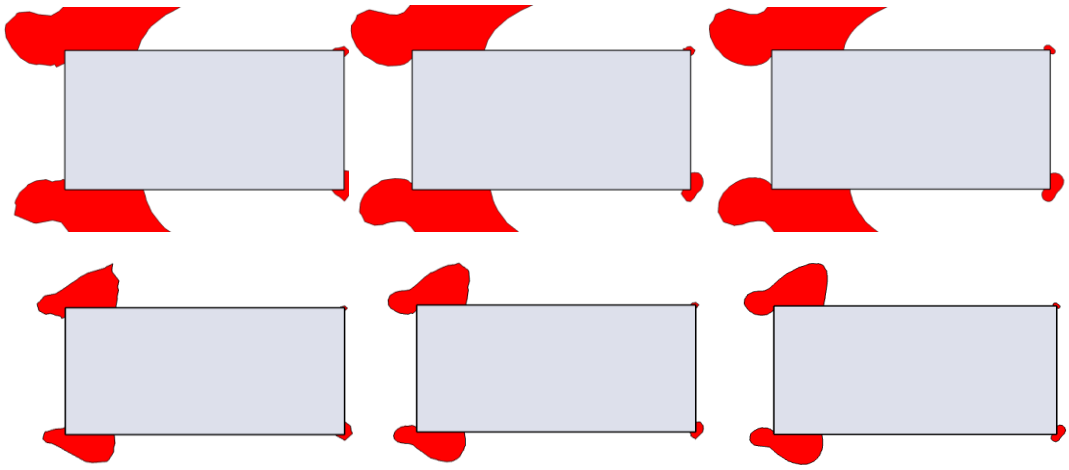

Figure 22: Model 1, Yield Areas around the Opening for S235JR (Top) & S355JR (Bottom)

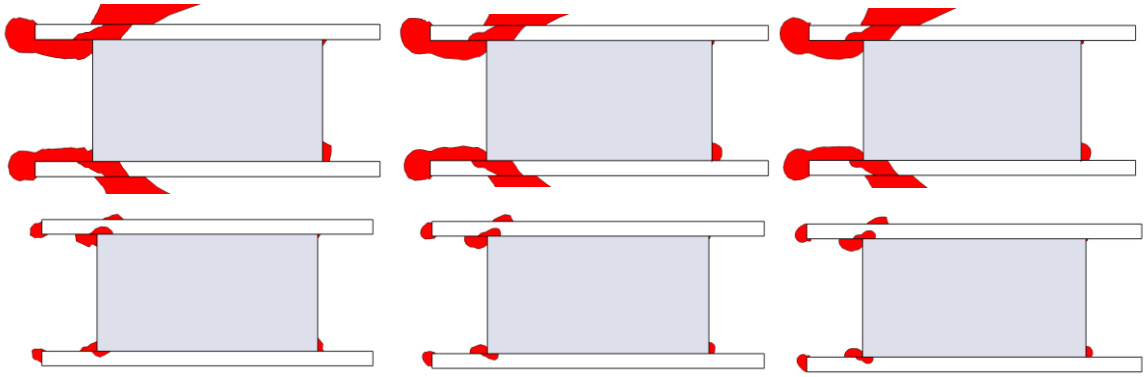

Figure 23: Model 2, Yield Areas around the Opening for S235JR (Top) & S355JR (Bottom)

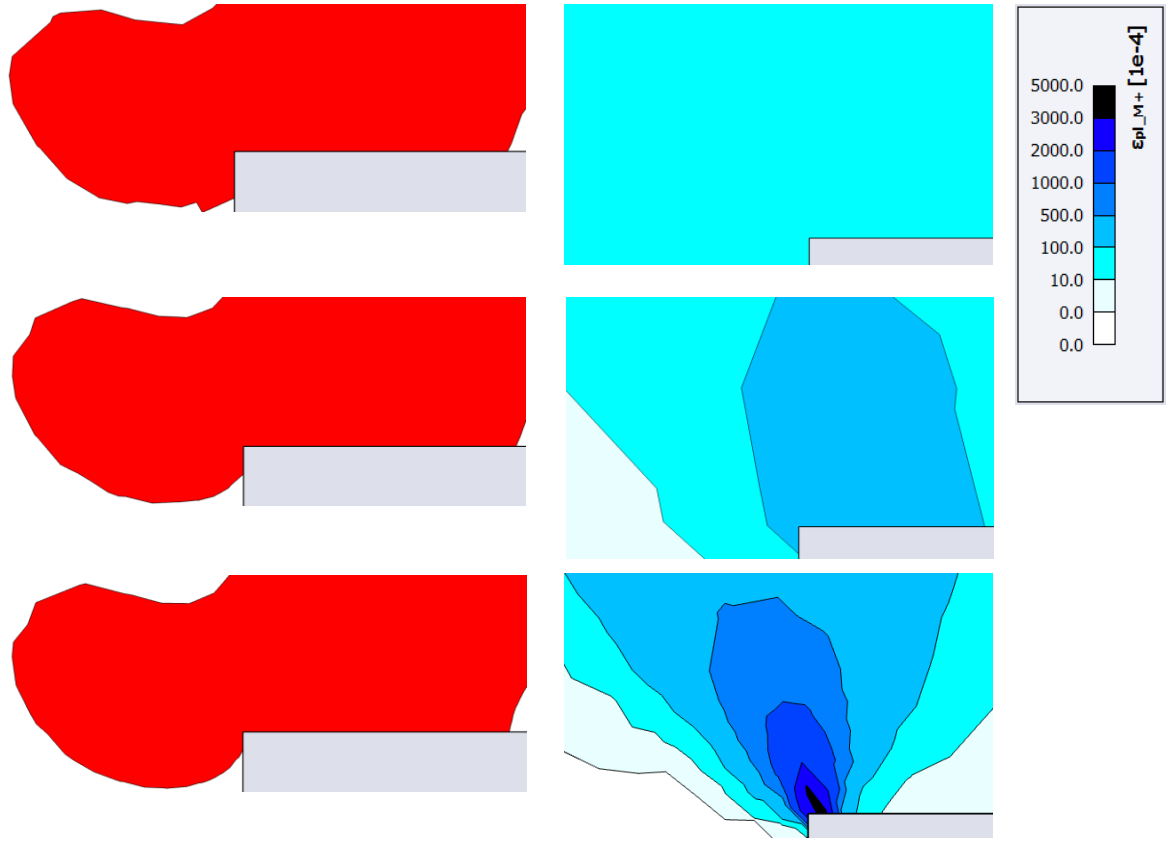

Figure 24: Model 1, S235JR Yield Stress Area (Left) & Equivalent Plastic Strain (Right)

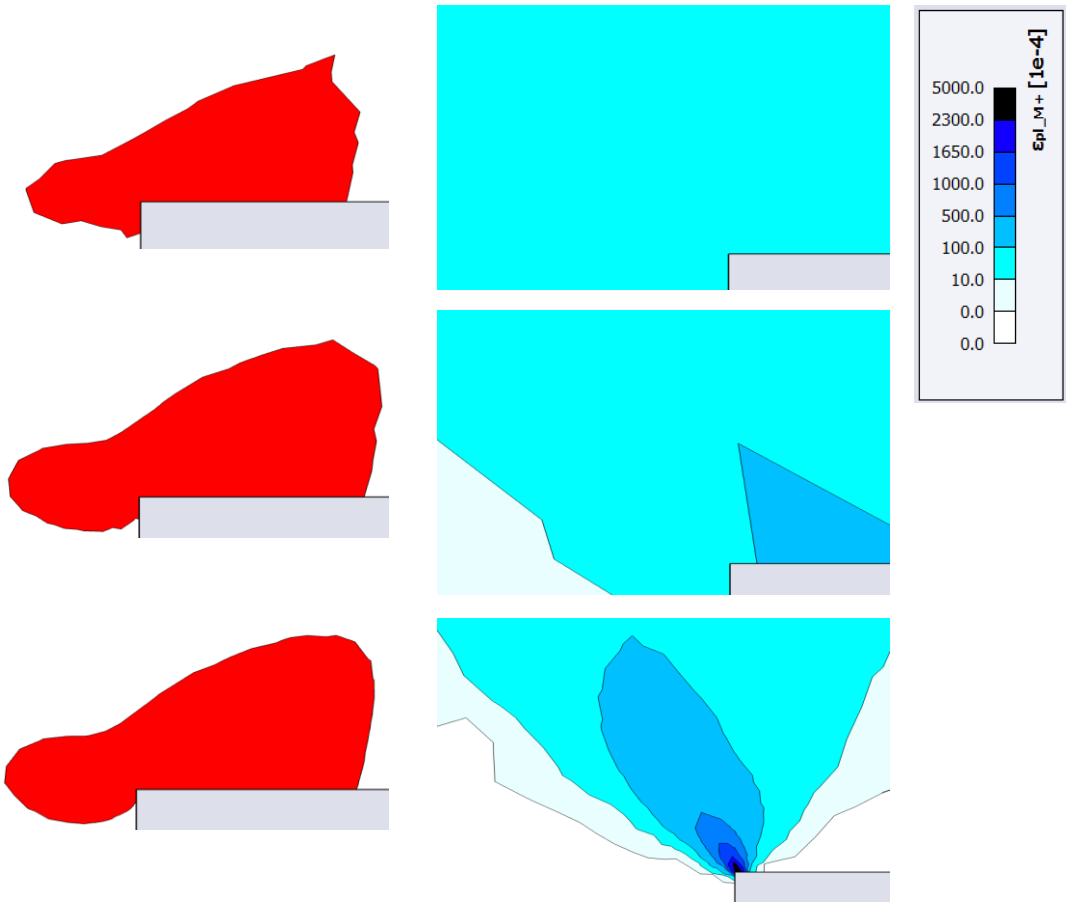

Figure 25: Model 1, S355JR Yield Stress Area (Left) & Equivalent Plastic Strain (Right)

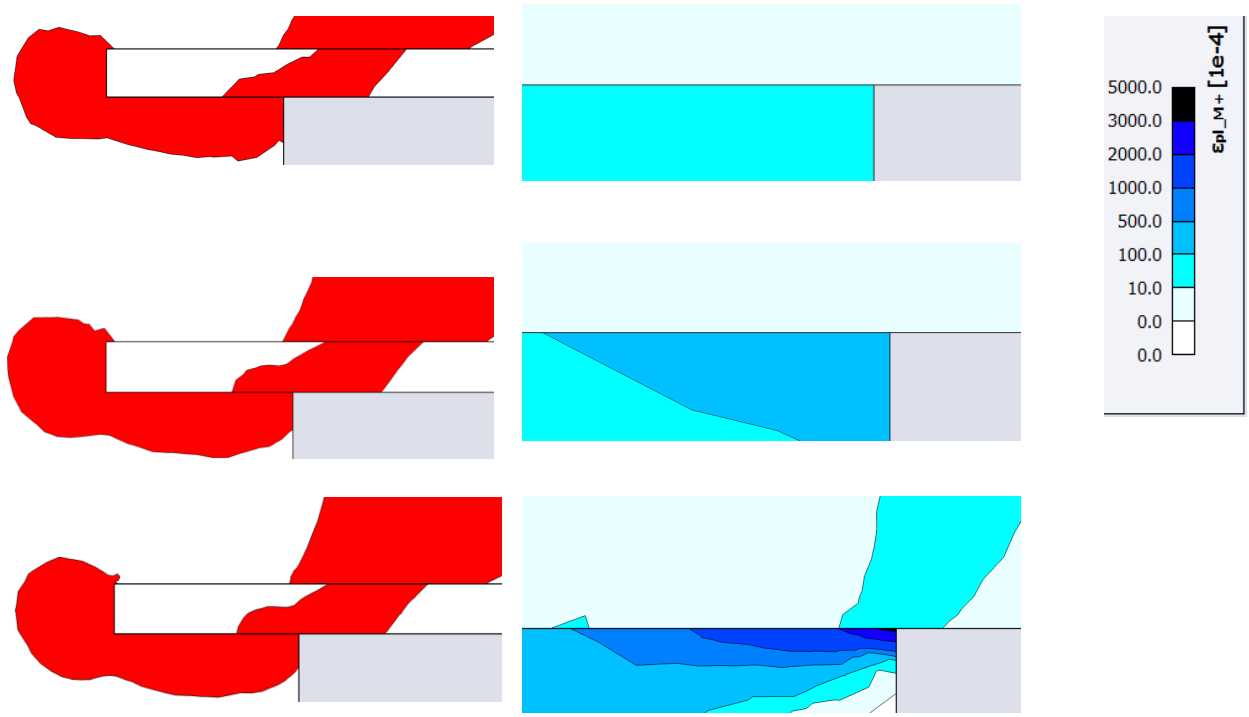

Figure 26: Model 2, S235JR Yield Stress Area (Left) & Equivalent Plastic Strain (Right)

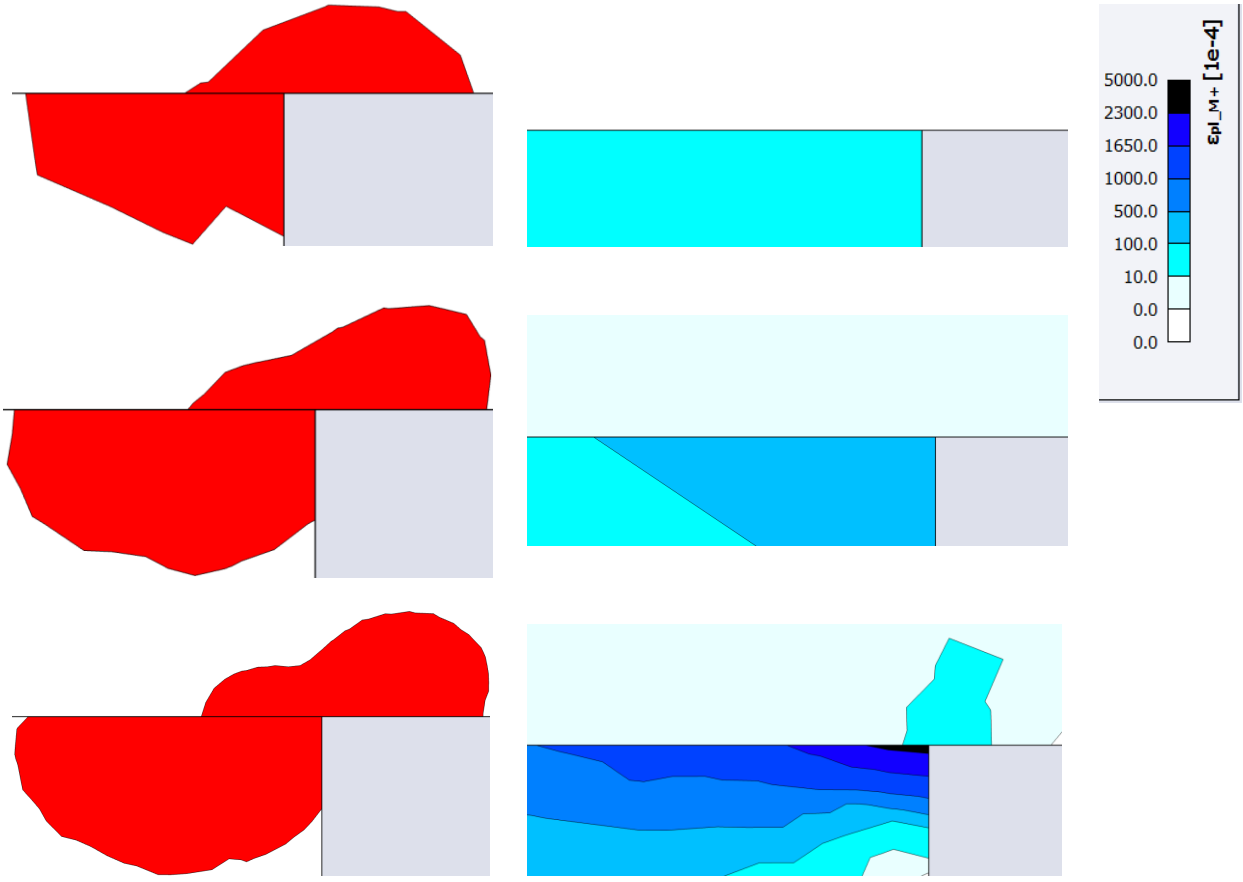

Figure 27: Model 2, S355JR Yield Stress Area (Left) & Equivalent Plastic Strain (Right)

From Figure 22 and Appendix C it can be observed that even though the S235JR steel fails in both models, the entire cross section of the critical area has surpassed the yield stress, resulting in a continuous yield surface. This makes calculating the yield area and local unity check value redundant for S235JR steel for both models. The S355JR steel however, does not yield across the entire cross section. Hence the yielding area and unity check value are to be calculated. As described the surface area where the material yields is calculated by manually counting the amount of elements per average element size group. The different distinctions for each refinement model and the following geometric properties are shown in Appendix D. Note that using the results case 'in centres' provides an overestimate of the actual surface area. Comparing the yield area using 'in centres' to using 'in nodes avg on macro' shows a small difference near the edges of the yield area. This is a safe estimation as the calculated yield area will be larger than the actual yield area as can be seen in Figure 28. The final surface areas are denoted in mm^2 in Table 3 rounded down to the last 2 decimals.

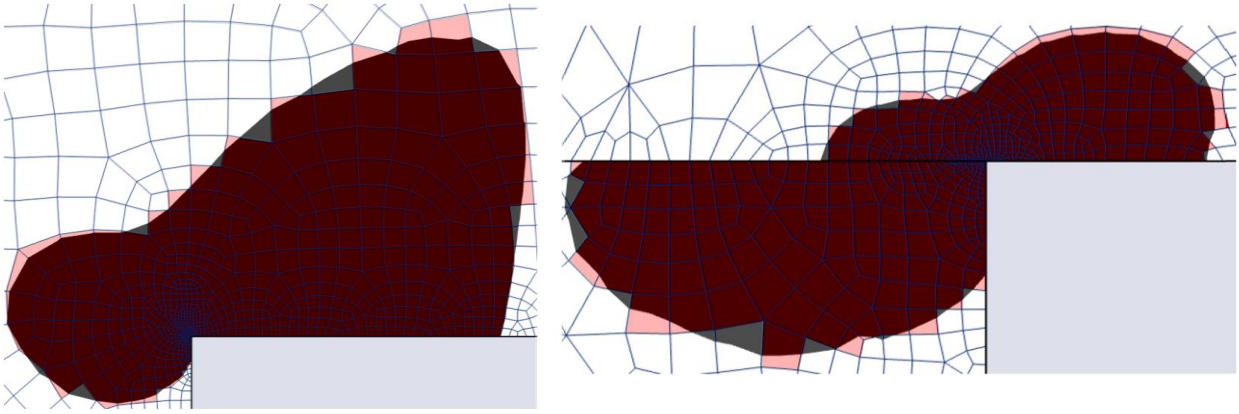

Figure 28: Yield Area Comparison of In Centres (Red) and Nodes avg on Macro (Black) for Model 1 (Left) & Model 2 (Right)

	Mesh 1	***Mesh 2***	***Mesh 3***
Model 1	4763,78	6154,17	7091,82
Model 2	1092,51	1107,07	1335,20

Table 3: Yield Area for Each Model and Mesh in mm^2

From Table 3 it can be seen
The corresponding equivalent stresses are derived from the in centres results case and shown in numbers for each element as can be seen in Figure 29. The resulting unity check values are based on the element with the highest equivalent stress and are shown in Table 5.

	Mesh 1	***Mesh 2***	***Mesh 3***
Model 1	2,38	3,19	10,56
Model 2	1,93	3,11	10,88

Table 4: Unity Check Values for each Model and Mesh

The discrepancies in found yield areas between mesh configurations 1 and 2 in relation to mesh configuration 3 are shown in Table 5

	Mesh 1	***Mesh 2***
Model 1	1,49	1,15
Model 2	1,22	1,2

Table 5: Differences in Yield Areas Between Mesh Configurations in Relation to Mesh 3



Figure 29: S355JR Stress Values at Failure for Model 1 (Top) and Model 2 (Bottom)

5 Discussion

This report has focused on a specific loading case for the beam with standardized dimensions for the beam, opening and its reinforcement. Doing so allowed for a side-by-side comparison between the standard beam and the reinforced beam regarding its linear elastic and nonlinear plastic behaviour. First some potential improvements on the applied methodology in this report will be addressed after which potential future works will be elaborated upon.

5.1 Model and Methodology

The model that eventually ended up being used in the report was not the first model attempted, in fact I tried different loading types, spans, heights and thicknesses of the beam. I settled on these loads and dimensions as to reflect realistic beam dimensions while still being able to obtain relevant plastic results. Experimenting allowed for some interesting insights, which albeit partly speculative, do allow for some insights in adjustments to the used methodology. Most notable would be the behaviour of the supports in response to varying load cases and to the increase of said loads. For example, when applying a uniformly distributed load the supports would often end up failing before the corners around the opening would. Reducing the span length and/or increasing the web thickness would allow for the beam to fail around the opening first instead. Doing so however, would mean the model no longer represented realistic beam proportions. Even though applying a point load instead of a uniformly distributed load or trapezium load resulted in the steel failing around the opening, the resulting linear elastic calculations consistently showed a plastic hinge occurring. To fix this, stronger steel types could be used, but doing so begs the question whether the results found would be useful for real life application.

From this the question arises whether attempting to simulate a beam in the first place is relevant for plastic analysis if it does not aim to research plastic hinges. Initially doing so was to create a realistic yield area due to bending. Achieving failure using a much smaller span would require a loading case that is not bending. Using a different loading type is not irrelevant, especially not when only looking at plates. But generally speaking beams are most commonly loaded in bending and are more likely to fail due to deformation rather than due to shear forces for example.

Regarding the applied methodology to find the yield area in each scenario ended up becoming an approximation rather than an exact value derived from the program's provided data. I do believe it is possible to achieve this. A method to do so would be to run an algorithm which takes the raw geometrical data of the nodes and finds which nodes belong to each element. After this the same formula can be applied to each element resulting in an exact yield area. I attempted to implement this, but found that the code was still running 2 days after executing it for the most refined mesh. If the operation complexity can be narrowed down applying this method would be a great improvement. This would also allow for a comparison between more models analysing different boundary conditions.

5.2 Future Works

For future research, looking into varying dimensions for the beam, opening and reinforcement, or looking into varying load applications, would allow for a better understanding of this relation between yield area and plastic behaviour. Doing so could potentially allow for generalized conclusions regarding whether or not the linear elastic yield area results in material failure. Additionally, aiming to further relate rough mesh results to very refined mesh results by identifying a limiting unity check value could also yield useful results.

6 Conclusion

This chapter evaluates the impact of the reinforcement on the found yield areas and plastic strains by answering the sub-questions posed in the introduction. After which, the main research question will be answered.

"*How large can the yield area and unity check value be before failure happens for both models and each mesh configuration?"*
As shown in chapter 4.2 no identifiable yield area could be derived from the results of the S235JR models, the S355JR models however, show that the yield areas and resulting unity check values can be rather large before failure happens. The smallest result being yield areas of 4763,78 and 1092,51 mm^2 and unity check values of 2,38 and 1,93 for model 1 and 2 respectively. The unity check values being large however, is mostly due to the small element size causing the linear elastic calculations to yield unrealistic results as can be seen from the same chapter where nearby elements bear much smaller equivalent stresses. When using a more refined mesh such as mesh 3, the unity check values become incredibly large (10,56 and 10,88), such that no reasonable conclusion can be derived from these findings. The yield areas however, do not suffer from this issue to such an extent. The yield areas for the most refined mesh configurations are equal to 7091,82 and 1335,20 mm^2 for model 1 and 2 respectively. Do note that these yield areas are an approximation of the actual yield area and most likely estimate this area to be larger than it would be in reality.

"What is the difference in yield area between models for each mesh size?"
A significant reduction in yield area can be observed between the standard model and reinforced model. On average the surface yield area decreased by ~80,3% for S355JR steel between the models for each mesh size. Presumably this happens due to the reinforcement supressing the yield area from expanding upwards. This finding implies that applying reinforcement to the opening allows a steel beam to bear greater loads without the cross section at the opening turning into a plastic hinge. Even though this problem did persist for the current models using S235JR steel, applying reinforcement would allow stronger steels to support larger openings over a greater span without turning into a plastic hinge.
Additionally, applying the reinforcement resulted in yield areas forming in places other than the observed critical corner. Extrapolating this finding implies that the stresses in said critical corner will no longer be the failure mechanism if the reinforcement thickness becomes sufficiently larger than the web thickness.

"What is the difference in plastic behaviour between models for each mesh size?"
Between the models the plastic behaviour appears to be restrained by the application of the reinforcement. Similarly to the yield area the plastic deformation 'grows' along the edge of the reinforcement until the material fails. Additionally the plastic deformation seems to be less concentrated when applying the reinforcement, i.e. the plastic strain reaches a greater value in a larger area relative to the area with the largest strain before failing.
To accurately describe plastic strain a very refined mesh appears to be required. Both models only showed critical plastic strain when using mesh configuration 3. The less refined meshes showed very little detail and practically no critical plastic strain.

"What mesh size provides sufficiently accurate linear elastic calculation results such that failure can be determined without a nonlinear calculation?"
From the determined yielding areas found using different meshes it is evident that the least refined mesh yields inaccurate results when it comes to stress distribution. The found yield area for model 1 is 1,49 times as small when using this mesh compared to using the most refined mesh. Model 2 yields a similar

discrepancy of 1,22. When looking at the medium sized mesh the yield areas have a much smaller discrepancy compared to the most refined mesh: 1,15 and 1,2 for model 1 and 2 respectively.

Now to return to the main research question: **"*What is the impact of applying reinforcement to a rectangular opening in a steel beam on the yield area and plastic behaviour at failure?*"**

Adding reinforcement greatly reduces the yield area and the shape of the yield area at failure. While reducing the concentration at which the plastic deformation develops. The smaller yield area at failure causes the beam to be able to support larger openings relative to increased loading without the cross section around the opening turning into a plastic hinge.

7 References

Chen, H. (2020). *Fundamentals of Finite Element Method.* Retrieved from phdonline.com: https://pdhonline.com/courses/s272/s272content.pdf

Crawford, R. J. (1998). CHAPTER 2 - Mechanical Behaviour of Plastics. In *PLASTICS ENGINEERING* (3rd ed., pp. 41-167). Elsevier Ltd. doi:10.1016/B978-0-7506-3764-0.50016-9

Hoogenboom, P. (2007, March 14). *Piekspanningen in eindige-elementenberekeningen.* Retrieved from phoogenboom.nl: https://phoogenboom.nl/CT5060_piekspanningen.pdf

Hoogenboom, P. (2024). *Notes on Shell Structures.* Retrieved from https://phoogenboom.nl/b17_book.pdf

Jafari, M., & Ardalani, E. (2016, February). Stress concentration in finite metallic plates with regular holes. *International Journal of Mechanical Sciences, 106*, 220-230. doi:10.1016/j.ijmecsci.2015.12.022

Kelly, P. (2010, July 8). 8.7 Associated and Non-associated Flow Rules. Auckland. Retrieved from https://pkel015.connect.amazon.auckland.ac.nz/SolidMechanicsBooks/Part_II/08_Plasticity/08_Plasticity_01_Introduction.pdf

Lee, C. (2023, November 14). *How Accurate is Laser Cutting: Standard Laser Cutting Tolerances*. Retrieved May 26, 2026, from ACCURL: https://www.accurl.com/blog/laser-cutting-accuracy/

Lemaitre, J. (1985a). A Continuous Damage Mechanics Model for Ductile Fracture. *Journal of Engineering Materials And Technology, 107*(1), 83-89. doi:10.1115/1.3225775

Lemaitre, J. (1985b). Coupled elasto-plasticity and damage constitutive equations. *Computer Methods in Applied Mechanics and Engineering, 51*(1-3), 31-49. doi:10.1016/0045-7825(85)90026-X

Li, Y., Lee, C.-C., & Cai, Y. (2023). Recent Research Advances in High-Performance Steel Tubular Members: Material Properties, Stub Columns, and Beams. *Buildings, 13*(11). doi:10.3390/buildings13112713

Motok, M. D. (1997). Stress concentration on the contour of a plate opening of an arbitrary corner radius of curvature. In *Marine Structures* (Vol. 10, pp. 1-12). doi:10.1016/S0951-8339(96)00012-3

Ohring, M. (1995). Engineering Materials Science. Academic Press, INC. Retrieved from https://www.google.nl/books/edition/Engineering_Materials_Science/LcvgiCbOo38C?hl=nl&gbpv=1&dq=inauthor:%22Milton+Ohring%22&printsec=frontcover

SCIA Engineer. (n.d.-a). *Calculations in SCIA Engineer: Types of analysis, FE mesh, Soil-In, Seismicity, Plasticity, AutoDesign, Optimisation.* Retrieved from https://help.scia.net/download/18.0/en/Calculations_enu.pdf

SCIA Engineer. (n.d.-b). *Nonlinear Calculation*. Retrieved from https://kc.scia.net/Help/kik/calculation/nonlinear_analysis/nonlinear_analysis.htm

Sönnerlind, H. (2015, June 3). *Singularities in Finite Element Models: Dealing with Red Spots*. Retrieved from COMSOL: https://www.comsol.com/blogs/singularities-in-finite-element-models-dealing-with-red-spots

Trott, M. (2026, March 25). *Singularity*. Retrieved from Wolfram Mathworld: https://mathworld.wolfram.com/Singularity.html#:~:text=Singularities%20can%20be%20classified%20as:%20*%20**Isolated,*%20**Irregular%20singularities**%20These%20are%20points%20where:

Vellaichamy, P., Vignesh, P., Indhumathi, L., & Senthilkumar, V. (2020). *Parametric studies on thin plates with holes.* IOP Conference Series: Materials Science and Engineering. doi:10.1088/1757-899X/764/1/012017

Vuik, C., Vermolen, F. J., van Gijzen, M. B., & Vuik, M. J. (2023). *Numerical Methods for Ordinary DIfferential Equations* (2 ed.). TUDelft Open. doi:10.5074/t.2023.001

Yoshida, K. (2017). A plastic flow rule representing corner effects predicted by rate-independent crystal plasticity. *International Journal of Solids and Structures, 120*, 213-225. doi:10.1016/j.ijsolstr.2017.05.004

Appendix A: Steel Properties

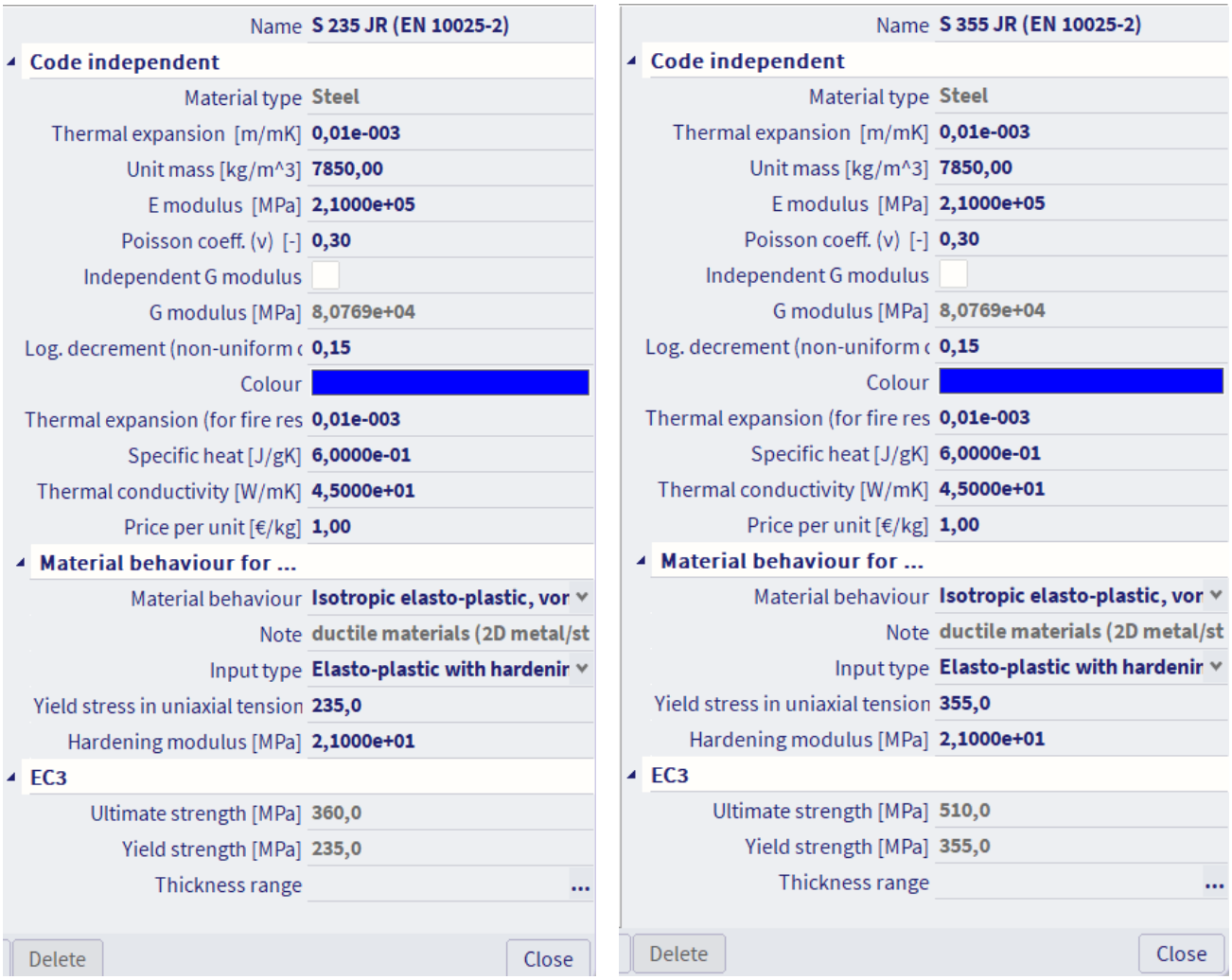

A.1: Steel Properties

Appendix B: Mesh Grids

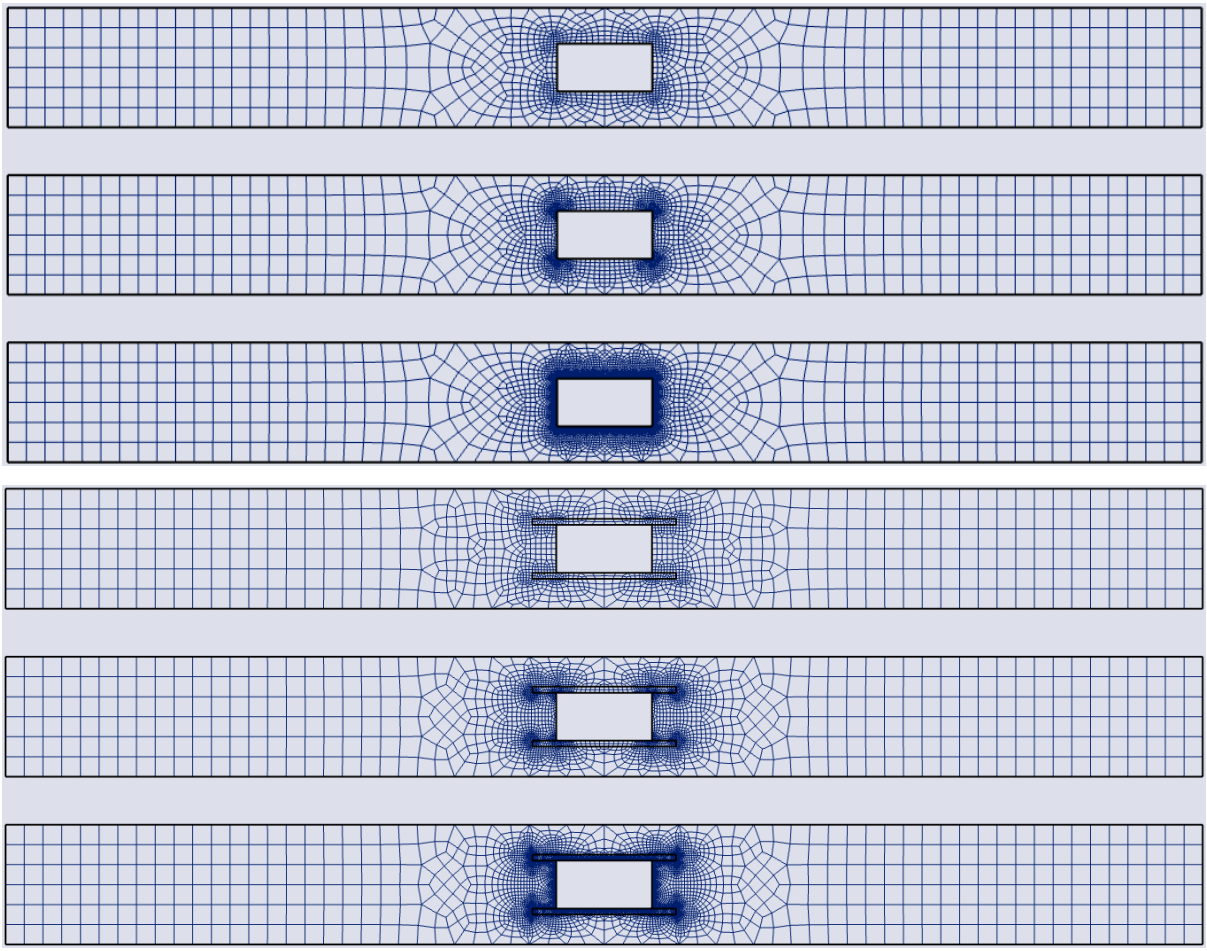

B.1: Mesh Configuration for Each Refinement

Appendix C: Yield Area & Plastic Strain of the Entire Beam

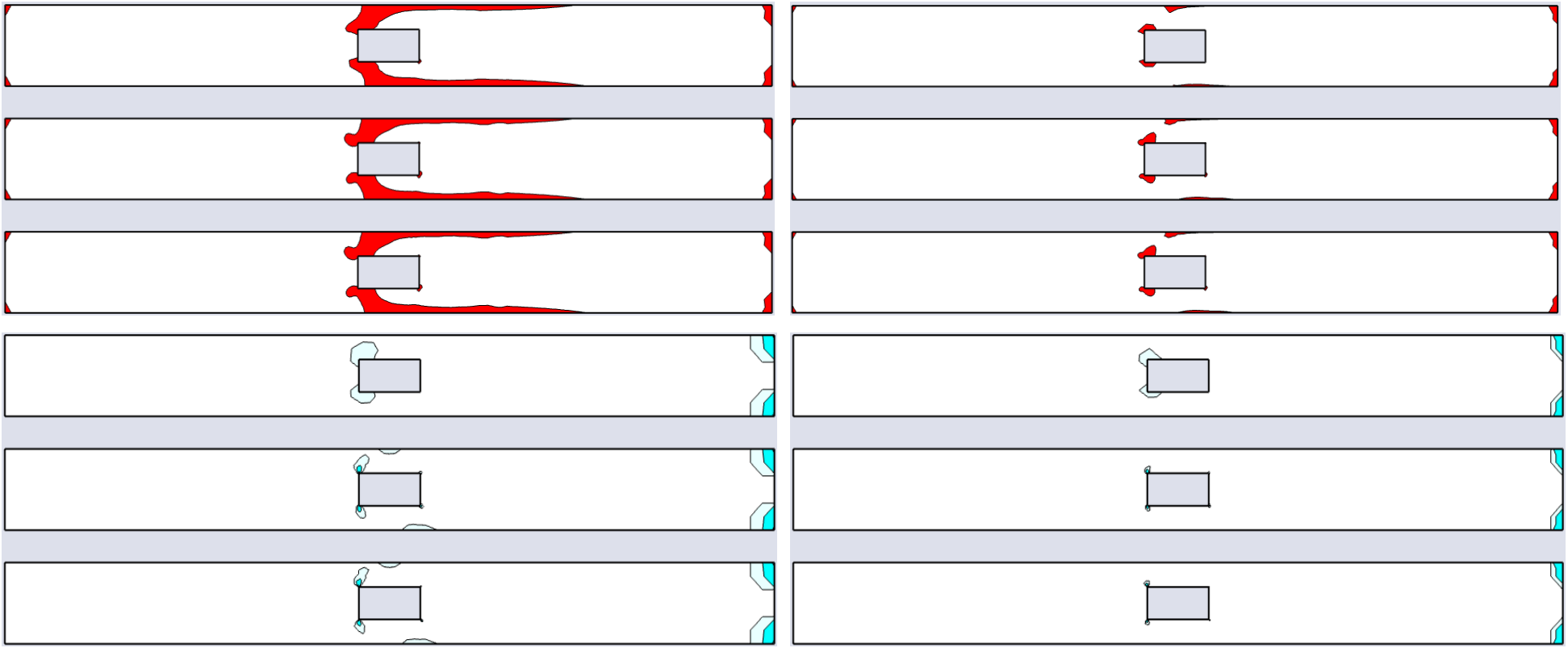

C. 1: Model 1 Equivalent Stress (Top) and Plastic Strain (Bottom) for S235JR (Left) and S355JR (Right)

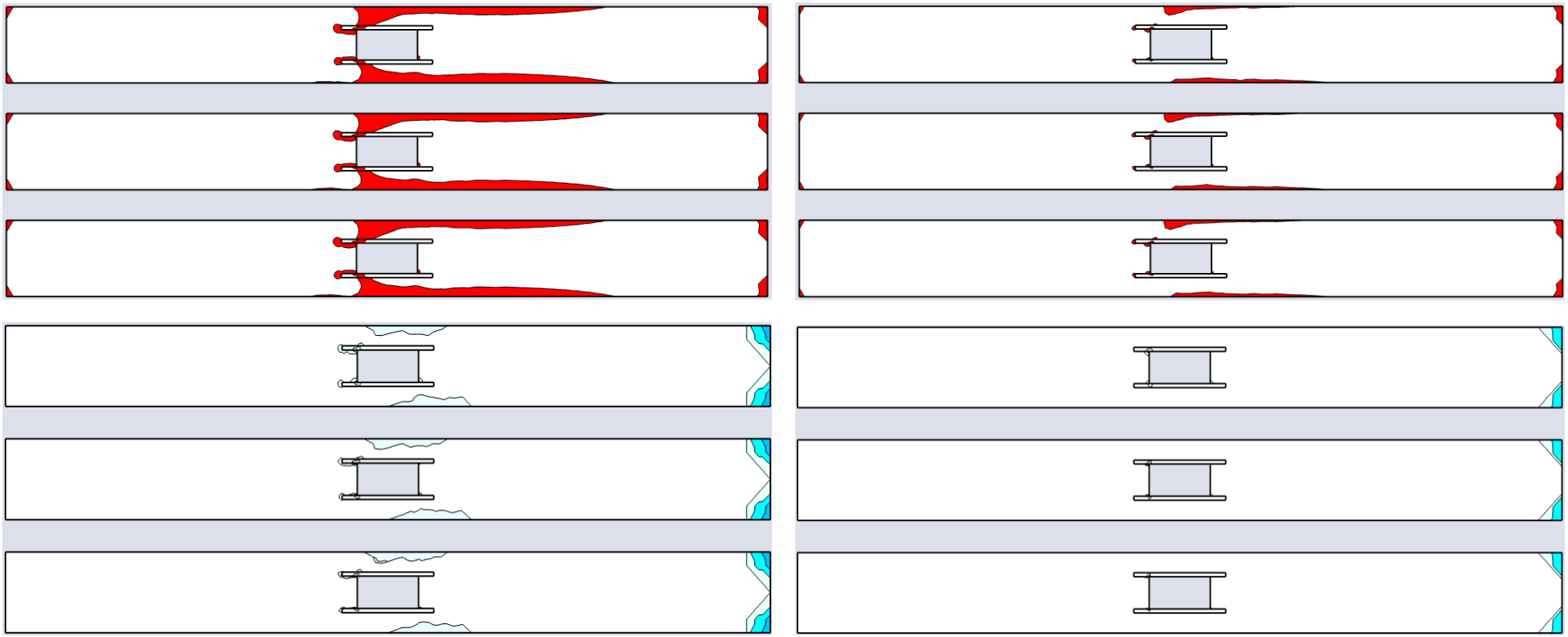

C. 2: Model 2 Equivalent Stress (Top) and Plastic Strain (Bottom) for S235JR (Left) and S355JR (Right)

Appendix D: Yield Area Division & Results

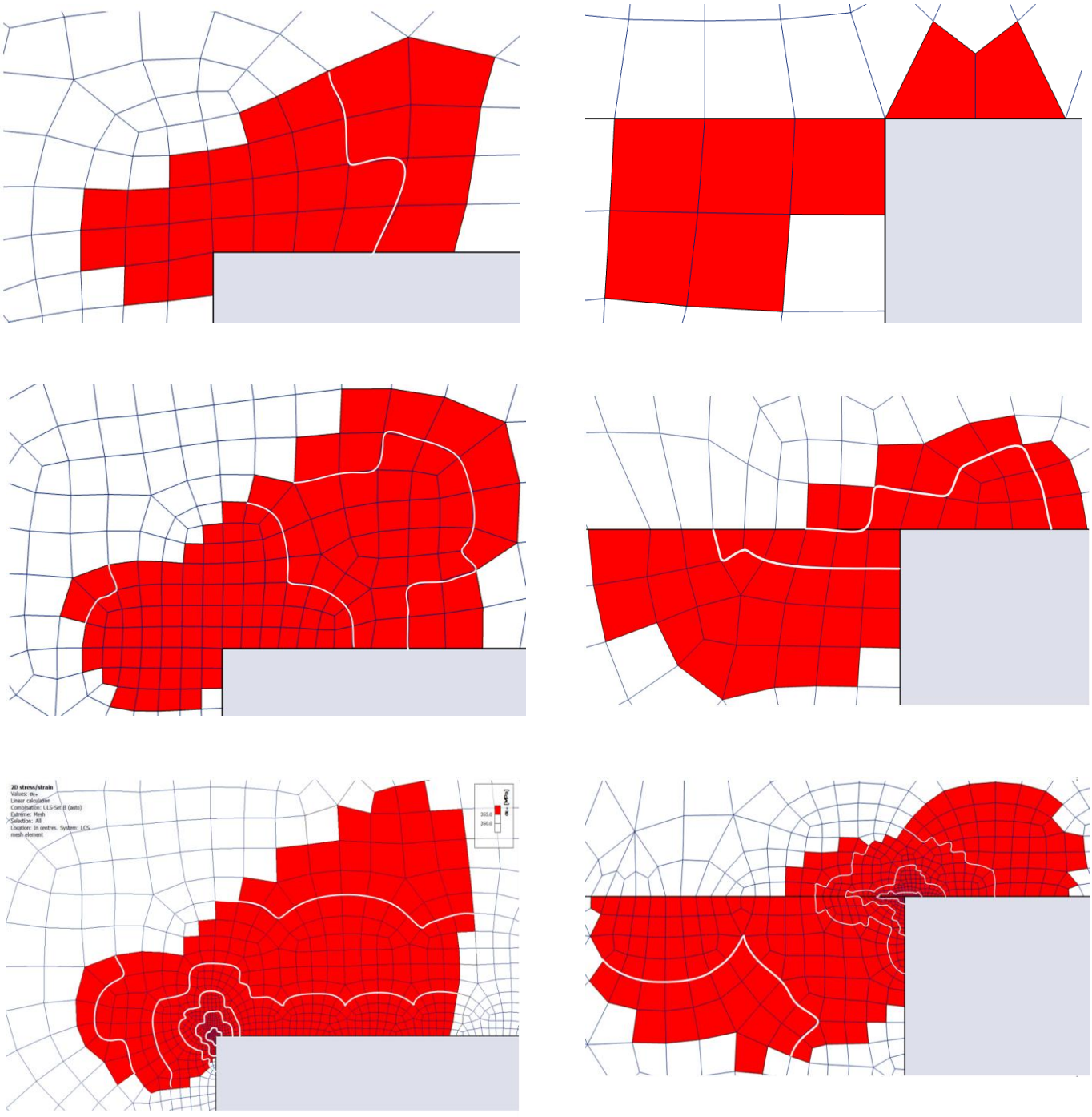

D. 1: S355JR In Centres Results Case with Element Size Distinction for Model 1 (Left) and Model 2 (Right)

Element Size:	Average Element Length [mm]	Average Area per Element [mm2]	Amount of Elements	Total Area [mm2]
1	11,44620898	131,0157	22	2882,3454
2	17,70796149	313,5719	6	1881,4314

Element Size:	Average Element Length [mm]	Average Area per Element [mm2]	Amount of Elements	Total Area [mm2]
1	5,377694674	28,91960001	76	2197,8896
2	8,075515463	65,21394999	31	2021,63245
3	11,75538175	138,189	14	1934,646

Element Size:	Average Element Length [mm]	Average Area per Element [mm2]	Amount of Elements	Total Area [mm2]
1	0,126688575	0,016049995	79	1,267949614
2	0,60095757	0,361150001	128	46,22720007
3	1,1461239	1,313599995	92	120,8511995
4	2,543157487	6,467650003	226	1461,688901
5	4,752430957	22,5856	122	2755,4432
6	9,343513793	87,30125001	31	2706,33875

Element Size:	Average Element Length [mm]	Average Area per Element [mm2]	Amount of Elements	Total Area [mm2]
1	12,49291399	156,0729	7	1092,5103

Element Size:	Average Element Length [mm]	Average Area per Element [mm2]	Amount of Elements	Total Area [mm2]
1	4,140259653	17,14174999	16	274,2679999
2	5,101470376	26,025	32	832,7999999

Element Size:	Average Element Length [mm]	Average Area per Element [mm2]	Amount of Elements	Total Area [mm2]
1	0,246170675	0,060600001	61	3,696600089
2	0,419821388	0,176249998	109	19,21124975
3	1,233045013	1,520400005	130	197,6520007
4	2,61608486	6,843899996	137	937,6142995
5	3,226918034	10,413	17	177,021

D. 2: Excel Tables for Model 1 (Top) & Model 2 (Bottom) for each Mesh